An ImageJ tool for simplified post-treatment of TEM phase contrast images (SPCI)

Amandine Verguet, Cédric Messaoudi, Marco Sergio, Patricia Donnadieu

Micron 121 (2019) 90–98

Contents lists available at ScienceDirect

Micron

journal homepage: www.elsevier.com/locate/micron

Short communication

An ImageJ tool for simplified post-treatment of TEM phase contrast images (SPCI)

Verguet Amandine[a,b,c,*], Messaoudi Cédric[b,c], Marco Sergio[b,c,d], Donnadieu Patricia[e]

[a] JEOL (Europe) SAS, allée de Giverny, F-78290 Croissy-sur-Seine, France
[b] Institut Curie, PSL Research University, CNRS UMR9187, F-91405 Orsay, France
[c] Université Paris-Sud, Université Paris-Saclay, INSERM U1196, F-91405 Orsay, France
[d] Sanofi Pasteur, avenue Marcel Merieux, F-69280 Marcy L'Etoile, France
[e] Univ. Grenoble Alpes, CNRS, Grenoble INP, SIMaP, F-38000 Grenoble, France

ARTICLE INFO

Keywords:
Image processing
Phase-contrast
Phase image
TEM image
ImageJ plugin

ABSTRACT

Tools for taking advantage of phase-contrast in transmission electron microscopy are of great interest for both biological and material sciences studies as shown by the recent use of phase plates and the development of holography. Nevertheless, these tools most often require highly qualified experts and access to advanced equipment that can only be considered after preliminary investigations. Here we propose to address this issue by the development of an ImageJ plugin that allow the retrieval of a phase image by simple numerical treatment applied to two defocused images. This treatment based on Tikhonov regularization requires the adjustment of a single parameter. Moreover, it is possible to use this approach on one-image. Although in that case the retrieved image gives only qualitative information, it is able to enhance the image contrast appropriately. This can be of interest for specimens producing low contrast images under the electron microscopes, such as some frozen hydrated biological samples or those sensible to electron radiation unsuitable for holographic studies.

1. Introduction

Characterization of nanometric objects is becoming crucial to address environmental and technological problems in biology (*i.e.*, asbestos contamination, nano-particle toxicity, vaccine adjuvants) and material sciences (*i.e.*, catalyst efficiency, compaction and material properties enhancement). Because Transmission Electron Microscopy (TEM) has high spatial resolution, it is the method of choice to address these issues. However, due to their size and low average atomic number some objects give rise to a low contrast impeding their differentiation from the background. With appropriate focusing of the objective lens, this so-called phase-contrast makes possible to highlight objects borders and structures otherwise invisible. Therefore, application of phase-contrast on nanometric objects can facilitate their study because it became easier to recognize them on a background. There is a drawback tough, as on the phase-contrast image the object contour and thus the size change with the focusing of the objective lens. More generally, a phase-contrast image displays a partial view of the object.

The formation of phase-contrast image is accounted by the contrast transfer function (CTF) of the microscope, which acts as a spatial filter depending, among other parameters, on the focusing of the objective lens. As a result, the phase-contrast images recorded at a certain focus is built only with a part of all the spatial frequencies, thus making some structures undetectable. Therefore, to obtain a fully reliable image of the object it is required to combine the information coming from phase-contrast images acquired at different defocus values. It has been demonstrated by Schiske (Schiske, 2002) that it is possible to retrieve from a TEM focal series a phase image that stands as a reconstruction of the object. The accuracy of this reconstruction depends on the focus step: a series taken with a smaller focus step leads to a higher accuracy but implies larger number of recorded images. More recently, Van Dyck et al. (1996) and O'Keefe et al. (2001) have shown that quantitative phase image, at full resolution by focal series reconstruction, requires a large set of experimental images. However, such a requirement increases the risk to induce damages on the sample. Because, the total electron dose received by the specimen is proportional to the number of recorded images, the advantage of phase image reconstruction for samples sensible to high electron doses is limited. This is the case of frozen hydrated samples in biology that require electron dose lower than $15e^{-}/Å^{2}$ (Karuppasamy et al., 2011). Additionally, the combination of images acquired at different focus to perform a phase image reconstruction needs sophisticated algorithms including several

* Corresponding author. Institut Curie, Bat 112, Campus Universitaire, 91045 Orsay cedex, France
E-mail address: amandine.verguet@ssji.net (V. Amandine).

https://doi.org/10.1016/j.micron.2019.01.006
Received 28 November 2018; Received in revised form 18 January 2019; Accepted 18 January 2019
Available online 28 March 2019

corrections of misalignment and distortion (Koch, 2014) as well as a non-trivial adjustment of parameters, limiting the use of phase image reconstruction.

To fully appreciate the benefits of phase image reconstruction the development of a user-friendly method able to retrieve a phase image from a limited number of phase-contrast images is needed. Based on a method requiring two defocused images and a simple numerical treatment (Donnadieu et al., 2008), we have implemented a plugin able to perform a quantitative phase-contrast reconstruction in the widely used image processing software ImageJ (Schneider et al., 2012). Moreover, we have adapted this approach to compute a qualitative phase image reconstruction enhancing borders and structures by using only one-image. The method requires only basic knowledge of TEM image formation and standard TEM equipment operated by a TEM user.

2. Tikhonov solution for simple phase retrieval from two phase-contrast images

2.1. Background

In TEM imaging, phase-contrast is a weak contrast that arises from the phase shift of the electron wave traversing the sample. When the sample is very thin or non-crystalline or constituted of light atoms, diffraction and absorption effects being small, phase-contrast is currently the more relevant for image formation. As phase-contrast is sensitive to very fine scale details, phase imaging is in principle the most appropriate to give high resolution information. However, a TEM image does not display a phase image but the result of the transfer of the exit electron wave by the electron optics. In the phase object approximation, this can be conveniently written in the reciprocal space as follows:

$$\hat{I}(q, \Delta z) = I_0(1 - 2\hat{\Phi}(q)\sin(\pi\lambda\Delta z q^2 + \frac{Cs}{2}\lambda^3 q^4)) \quad (1)$$

where $\hat{I}(q)$ and $\hat{\Phi}(q)$ are respectively correspond to the Fourier Transform (FT) of $I(r)$, the intensity, and $\Phi(r)$, the phase function; I_0, the intensity of the incident wave; λ, the electron wave length; Δz, the objective lens defocus; Cs, the objective lens spherical aberration coefficient.

It is worth noting that the phase function $\Phi(r)$ represents the object (with the only bias of the projection effect), while the image $I(r)$ is modified by a CTF that depends on the imaging conditions, *i.e.* the electron wavelength and the objective lens characteristics (aberration coefficients, Δz). As proposed by Schiske (2002), the phase can be restored using a series of TEM images taken at different defocus. When the aim is to achieve a high resolution reconstruction, a large number of images and small defocus step are required. But if a limited resolution can be sufficient (for instance a resolution not better than 1 nm *i.e.* $q < 1\,\mathrm{nm}^{-1}$), the high order term can be neglected in relation that then writes as:

$$\hat{I}(q, \Delta z) = I_0(1 - 2\hat{\Phi}(q)\sin(\pi\lambda\Delta z q^2)) \quad (2)$$

As far as the term $\pi\lambda\Delta z q^2$ is small (*i.e.* ≈ 0.5), the sinus function can be approximated by its argument, relation (2) writes then as:

$$\hat{I}(q, \Delta z) = I_0(1 - 2\hat{\Phi}(q)\pi\lambda\Delta z q^2) \quad (3)$$

At this step, it should be noted that the previous approximation determines the resolution of the method since the condition $\pi\lambda\Delta z q^2 < 0.5$ corresponds in direct space, to dimensions larger than $\sqrt{2\pi\lambda\Delta z}$. As a consequence, the resolution of this simplified method depends on the experimental conditions, *i.e.* the wave length and the focus Δz. For example, at 200 keV, a focus $\Delta z = +50$ nm will give a phase image with a resolution limited to 1 nm by the method.

This simplified relation can be applied to two images recorded at $+\Delta z$ and $-\Delta z$ to derive a relation between the FT of the phase function $\hat{\Phi}(q)$ and $\Delta\hat{I}(q) = \hat{I}(q, +\Delta z) - \hat{I}(q, -\Delta z)$ the FT of the difference between these two images:

$$\hat{\Phi}(q) = -\frac{1}{I_0}\frac{1}{4\pi\lambda q^2}\frac{\Delta\hat{I}(q)}{\Delta z} \quad (4)$$

This relation has been here obtained using a CTF. However it has been also demonstrated from a more general point of view using a Transport Intensity Equation (TIE) (Paganin and Nugent, 1998) (Paganin and Nugent, 1998; Ishizuka and Allman, 2005). The advantage of the CTF approach is to be more familiar to TEM users.

It is worth noting that, instead of considering two images recorded at $+\Delta z$ and $-\Delta z$, following the relation (3), the phase could also have been simply derived from the image at zero focus and the image at focus Δz. In that case the phase is given by the following relation:

$$\hat{\Phi}(q) = -\frac{1}{I_0}\frac{1}{2\pi\lambda q^2}\frac{\Delta_0\hat{I}(q)}{\Delta z} \quad (5)$$

where $\Delta_0\hat{I}(q) = \hat{I}(q, \Delta z) - \hat{I}(q, 0)$ is the difference between the FT of the image recorded at focus Δz and the one at zero focus. Therefore, depending on the images available, either a numerical treatment based one TEM image and or a two-image treatments based on a focal series of two TEM images can be carried out. It has been done above using the CTF approach but can also be obtained with the TIE one. The respective advantages and limits of both treatments will be considered in the following.

2.2. Tikhonov regularization and the SPCI image treatments

The main issue to retrieve the phase function $\Phi(r)$ using relation (5) is to deal with the singularity in $q = 0$ arising from the function $1/q^2$. This difficulty, typical with inverse problems, can be solved using a Tikhonov regularization as proposed by Mitome et al. (2010). It means replacing the $1/q^2$ function by a function $T(q) = q^2/((q^2 + a^2)^2)$. For $q \gg a$, $T(q)$ is close to $1/q^2$ while for $q = 0$ and its vicinity, they strongly differ since $T(q)$ tends to 0 for $q = 0$ and is maximum for $q = a$.

The wave vector $q = 0$ and its vicinity correspond to low spatial frequencies domain in reciprocal space, *i.e.* long-scale fluctuations in direct space that are often due to meaningless contrast fluctuations. Therefore, depending on the scale of details of interest and of the meaningless information with respect to the region of interest, the impact of the regularization is variable. The above Tikhonov regularization provides a simple solution but one will have to be careful in the choice of the parameter a-value.

The strong point of this regularization method is to involve only one parameter. In general, the length scale of interest of a system is known, therefore making the appropriate choice should be easy. As illustrated in Fig. 1, in the vicinity of $q = 0$ the information will be cancelled out while for $q = a$, the Tikhonov function is maximum. This means that depending on the wave length of significant details with respect to this maximum, they might be cancelled out or rather amplified. In other words, it is extremely important to have in mind the characteristic wave length (either for the meaningful and meaningless details) to make a correct choice.

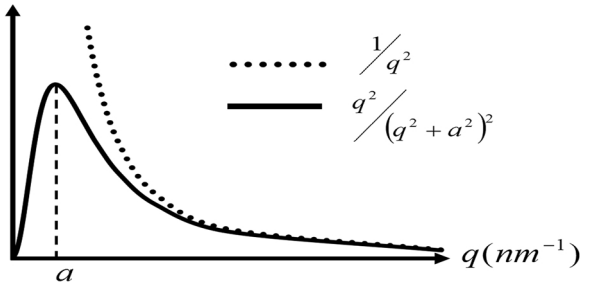

Fig. 1. Graphical representation comparing the function $1/q^2$ and a Tikhonov function $T(q) = q^2/((q^2 + a^2)^2)$.

The simplified approach described by relation (4) after implementation of the above Tikhonov regularization then consists in retrieving the phase image using the following relation:

$$\hat{\Phi}(q) = -\frac{1}{I_0}\frac{1}{4\pi\lambda}\frac{q^2}{(q^2+a^2)^2}\frac{\Delta\hat{I}(q)}{\Delta z} \quad (6)$$

At first it requires the acquisition of two images at focus $-\Delta z$ and $+\Delta z$. In the relation (6), I_0 stands for the intensity of the incident wave. In case of a weak phase object, I_0 is given by the image at zero focus, *i.e.* the zero-contrast image. However, if it can be assumed that the $I(+\Delta z)$ and $I(-\Delta z)$ images are showing phase-contrast, I_0 can be estimated from their background which has the advantage to limit the number of required images to two ($I(+\Delta z)$ and $I(-\Delta z)$). Considering this approximation in addition to the ones done on relation (3) (Section 2.1) allows to further simplify our approach of phase retrieval, referred to Simplified Phase Contrast Images (SPCI).

It should be noted that the same approximation on the zero-focus image can be applied to relation (5). The phase can be retrieved using only a single experimental image, *i.e.* a defocused image. In the following we will refer to two-images SPCI treatment when two images $I(+\Delta z)$ and $I(-\Delta z)$ are used, and to one-image SPCI treatment when only a defocused image is used; in both cases the zero-defocus image will be replaced by a constant background intensity image.

As the phase retrieval based on the Tikhonov regularization can be described as a filter in reciprocal space, the spatial frequencies being transferred according to the function $T(q)$, the numerical treatment can be seen as a simple image processing that can be achieved by many software. The processing will involve the experimental defocused images (either one or two if the one-image or two-images treatment is chosen, respectively) and two images build by the operator, *i.e.* the constant intensity image that will stand for the zero-focus image and an image in reciprocal space representing the Tikhonov function $T(q)$. In the present case, as described in the next section, it was chosen to write a plugin for the software ImageJ (Schneider et al., 2012).

Because of the image subtraction involved in the processing, the images $I(+\Delta z)$ and $I(-\Delta z)$ have to be properly aligned. Shift correction can be done using a plugin already available for ImageJ (Schneider et al., 2012) such as TomoJ software (Messaoudi, 2011). Also because of the focus difference, the images $I(+\Delta z)$ and $I(-\Delta z)$ may have slightly different magnification. This can occur for high focus, in such case a re-scaling should be done directly with ImageJ software. When nedded, image alignment and re-scaling should be done as a pre-treatment before retrieving the phase image.

Finally, it is worth noting that the output of the calculation is in radian, that providing the reciprocal scaling factor has been taken into account. For a N pixel ROI and a pixel size p in direct space, the pixel size in the reciprocal space is $1/Np$. Therefore, a multiplication by a factor N^2p^2 arises when the numerical calculation of the Tikhonov regularization function is done in reciprocal space pixel.

In this section we describe the implementation of the ImageJ plugin and its evaluation with gold nano-particle, trypanosome resin embedded and frozen hydrated bacteria as examples for material science and biological applications.

3. SPCI plugin: Workflow conception and interface

The algorithm behind SPCI plugin is composed of 3 major steps (Fig. 2). In the first step two aligned defocused images (Fig. 2A and B) are selected by the user. Some parameters, related to the microscope and described below, are then requested (Fig. 2C). In order to compute the phase image (Fig. 2F), an image of the Tikhonov parameter a-value (Fig. 2E) is generated to filter the result of the FT. Another image (Fig. 2D) is obtained from the subtraction of the two aligned defocused images, which result is divided by a background image or a zero contrast image. This step is explained in the previous section uses a background value or an image as I_0. The second step consists in taking the FT of the difference between the two defocused images (FT) and to multiply by the Tikhonov regularization (5), *i.e.* a computed image based on the function $q^2/(q^2+a^2)^2$ with q in pixel. The last step consists in computing the inverse FT (FT^{-1}) to obtain the phase map in direct space (Fig. 2F).

Experimental conditions (focus value, voltage or electron wavelength, pixel size) are provided by the user as well as background value from the selected focus images and the Tikhonov parameter. It should be noted that the user interface (Fig. 3) will require a-value in pixel (a) that will be transformed in reciprocal space units using the pixel size parameters and will be displayed in the interface window.

SPCI plugin has been developed in JAVA to be easily used with ImageJ (Schneider et al., 2012). ImageJ is a widely used tool for image processing and analysis. As Parallel colt JAVA library (Wendykier and Nagy, 2010) offers a better implementation of the FT than ImageJ, this library is used by SPCI. To warranty correct computation of contrast image it is required that the pixel (over and under-focused images) corresponds to equivalent positions on the sample. Indeed, phase-corrected image is calculated pixel per pixel by applying equations described in Section 2 and therefore for each image (over and under-focus) pixels might be aligned. `TomoJ` (Messaoudi et al., 2007) provides already plugins with robust algorithms for this purpose and there is also other plugin dedicated to the alignment, such as `TurboReg` (Thevenaz et al., 1998) and `Template Matching and Slice Alignment` (Tseng, 2018). We decided to not include this step in SPCI plugin.

SPCI plugin user interface starts by the selection of only two focused images ($+\Delta$ and $-\Delta$ symmetric with respect to zero focus) in input as well as the absolute value of their defocused, electron wavelength, and pixel size is required. It is also possible to include only one image and therefore only a qualitative approach will be applied. As described above, the interface offers the possibility to choose how the background is determined. This value or image will be used as I_0 in the equation. The interface require a Tikhonov a-value in pixel. Its equivalence in nm^{-1} is dynamically displayed. To help user to determine the appropriate a-value, the plugin offers to compute the phase image for several Tikhonov parameter or a-value in one run: the number of a variations and the multiplying factor between each variation are chosen by the user. For instance, for the above choice (Fig. 3), the user obtains 3 images with a-values of 10, 100, 1000 pixels.

4. Application of SPCI plugin to experimental data

4.1. Experimental details

To evaluate the capabilities of SPCI plugin for material science and biological applications, we have used gold nano-particles with size ranging between 1 and 5 nm deposited on carbon coated grid and *Trypanosoma brucei* semi-thin (200–300 nm) epon embedded section as well as frozen hydrated *Escherichia coli* K12 sample. TEM observations for gold nano-particle were carried out on a FEI Titan 80–300 with probe and image aberration corrector operated at 300 kV. No objective aperture was used for the TEM image formation. Brightness was adjusted to obtain a good signal-to-noise ratio and a short exposure time to avoid drift during image acquisition. Focal series were recorded on a Gatan slow scan CCD camera, at 185,000× magnification with defocus range from −200 to 200 nm and 20 nm defocus step between images. The zero-focus objective lens current was estimated as accurately as possible from the absence of contrast of the carbon supporting film.

Regarding biological samples, *T. brucei* was prepared as described in Trépout et al. (2018). In the case of frozen hydrated specimen, *E. coli* at initial stationary phase was diluted with LB culture medium. An aliquot of 5 µl was deposited on a 200 mesh copper lacey carbon grid and then frozen in liquid ethane at −178 °C by using Leica EM CPC and transferred to a JEOL Electron Microscope JEM-2200FS by using Gatan 626 high-tilt cryo-holder. Images were acquired at 200 kV using a 100 µm

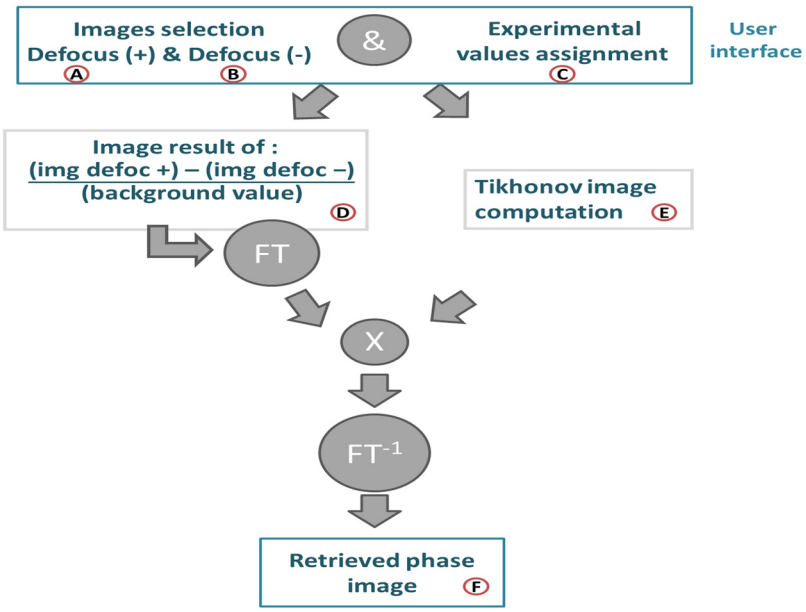

Fig. 2. SPCI workflow, the major steps of the algorithm are illustrated. A, B, C are selected in the interface by the user. The intermediate image D extracts information from the focus images. E is the image of the Tikhonov parameter. F is the phase image obtained at the end of the process. img, image; FT, Fourier Transform; FT^{-1}, Fourier Transform inverse.

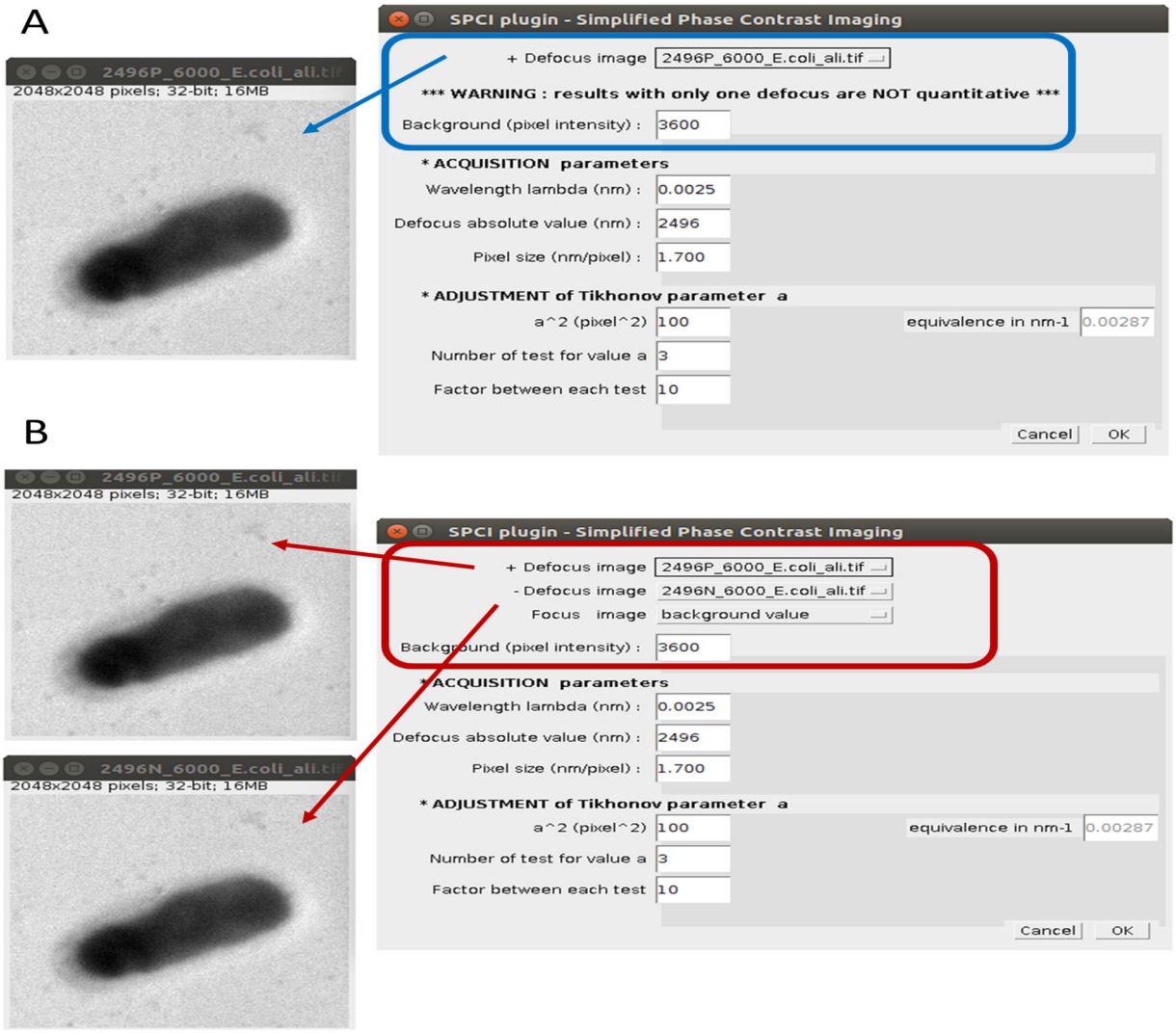

Fig. 3. Screenshot of the two possible user interfaces of SPCI plugin. In the first interface, a warning message notifies the user that the treatment with one-image is not quantitative. The one-image SPCI treatment is still possible from the multiple-image interface by selecting “background value” in the choice of second defocus image.

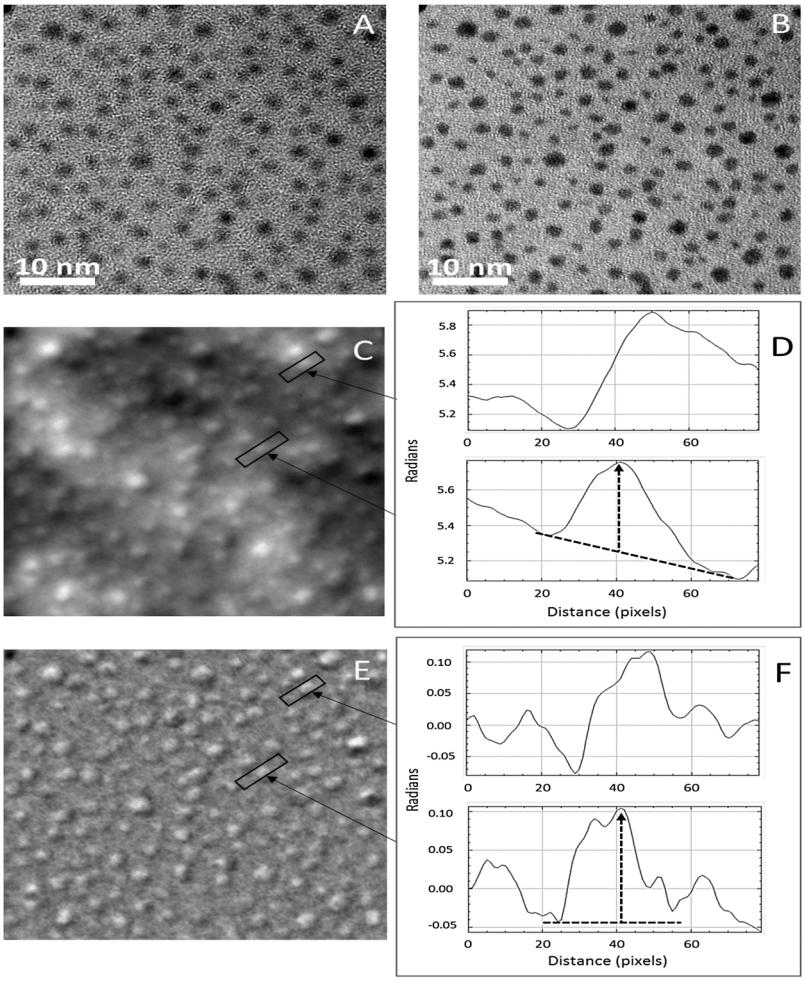

Fig. 4. Two-image SPCI treatment applied to gold nano-particle. A and B correspond to +40 nm and −40 nm defocus images, respectively. C and E are the phase image resulting from two-images SPCI treatments for Tikhonov value of $a = 1$ pixel and 10 pixels (corresponding in the image acquisition conditions to $a = 0.02\,\mathrm{nm}^{-1}$ and $a = 0.2\,\mathrm{nm}^{-1}$). Respectively, graphics D and F show the intensity profiles of the gold particles in the region of interest pointed by arrows on images C and E. As pointed by the dotted arrows, depending on the *a*-parameter, the measured phase values are respectively about 0.5 rad for $a = 1$ pixel ($0.02\,\mathrm{nm}^{-1}$) and about 0.1 rad for $a = 10$ pixels ($0.2\,\mathrm{nm}^{-1}$).

condenser aperture (CLA2). Acquisition was performed at a magnification between 8000 and 15,000× using a Gatan slow scan CCD US1000 camera with one second exposition time. Multi-scale cross-correlation alignment using TomoJ were used starting with binning 4 and integer translation.

4.2. Results

4.2.1. Test and validation of SPCI treatments on gold nano-particles

4.2.1.1. Quantitative approach using two symmetric defocused images. The gold nano-particles system is important for evaluating SPCI from a quantitative point of view while the other examples aim at illustrating its potential for biological systems.

Fig. 4 displays the phase image obtained with the two-images SPCI treatment from images of gold nano-particles recording at +40 nm and −40 nm. According to the relation between defocus and resolution, reported in Section 2.1, 40 nm defocus will give a retrieved phase image with appropriate resolution for particles within the range of 1–5 nm. Fig. 4 illustrates the influence of the Tikhonov parameter on the value given by the phase image. As shown in Fig. 4C and E, highlighted details strongly depend on the Tikhonov parameter, namely a higher contrast can be observed for $a = 0.2\,\mathrm{nm}^{-1}$. It should be noted that these profiles represent phase value in radian. For the Tikhonov parameter *a*-value $= 0.02\,\mathrm{nm}^{-1}$, the phase profiles indicate that the phase-shift corresponding to these particles is about 0.5 rad. For the Tikhonov parameter *a*-value $= 0.2\,\mathrm{nm}^{-1}$, the profiles indicate smaller values, of about 0.1 rad. As far as particles are concerned, the phase shift can be simply calculated from the particle size (t) and the mean inner potential V_0 using the relation $\Phi = \pi V_0 t/\lambda E$ (Reimer, 1989). According to the mean inner potential of gold nano-particles in this size range (Popescu et al., 2007) the expected phase-shift is about 0.6 rad. Therefore, the Tikhonov parameter $0.02\,\mathrm{nm}^{-1}$, with the numerical SPCI treatment which is the minimum one (corresponding to 1 pixel), gives the better match with the expected phase value. In other words, the two-images SPCI plugin is able to provide quantitative phase measurement when the Tikhonov parameter is set to its minimum. It is worth mentioning that the parameter a of the Tikhonov regularization can take any real value. But when dealing with images as above with the SPCI plug in, the a parameter necessarily corresponds to a number of pixels, the pixel unit being defined by the reciprocal space distance $1/Np$ where N is the number of pixel of the image and p the pixel size in direct space. So $a = 1$ pixel is the minimum Tikhonov parameter for the given acquisition conditions (*i.e.* TEM magnification, camera binning).

The drawback of this choice is that the image contrast is rather poor in comparison with the one obtained with higher Tikhonov parameter. This is rather obvious in Fig. 4E that contrast is improved by the SPCI treatment because the background is removed and particles remains. Furthermore, this is confirmed by the Weber–Fechner contrast (Trémeau et al., 2009) computed from the intensity profile (Fig. 4F). Briefly, this contrast measures the difference between the signal intensity and the background intensity normalized by the background intensity. This value increases 36 times between the Tikhonov *a*-value $= 0.02\,\mathrm{nm}^{-1}$ and *a*-value $= 0.2\,\mathrm{nm}^{-1}$. Therefore, depending on the desired application, the two-images SPCI treatment can be a tool for quantitative studies when minimum Tikhonov parameter is used or for qualitative analysis due to a better visualization of specific details by contrast increment. In this last case, SPCI plugin acts as an image filter to emphasize the object of interest.

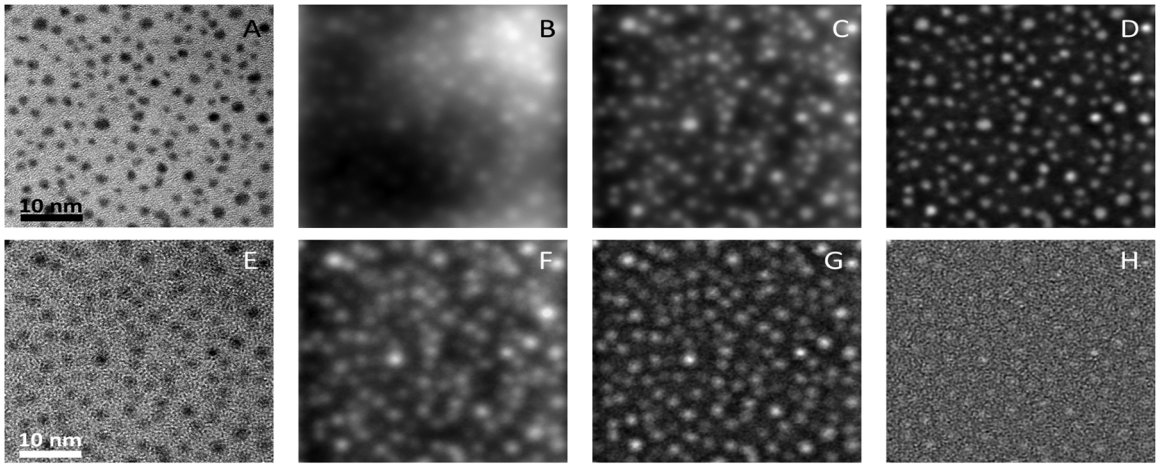

Fig. 5. One-image SPCI treatment applied to gold nano-particles. Figs. A and E show images of a same area recorded for focus images $\Delta z = -20$ nm and $\Delta z = +60$ nm respectively. Figs. B, C and D (respectively F, G, H) display the phase image retrieved with the one-image SPCI treatment from image A (respectively E) for various values of the Tikhonov parameter: $a = 0.06\,\mathrm{nm}^{-1}$; $a = 0.2\,\mathrm{nm}^{-1}$; $a = 0.6\,\mathrm{nm}^{-1}$. The scale bar on the original images A and E represents 10 nm.

The use of SPCI plugin as an image filter can be simplified with the requirement of a single image we described in the next section.

4.2.1.2. Qualitative approach using the one-image SPCI treatment. The one-image treatment implemented in SPCI plugin has been derived from the two-images one by replacing one of the two defocused images by a constant intensity image corresponding to the background value. As emphasized in the previous section, the one-image SPCI treatment is qualitative and cannot be compared to quantitative one-image phase retrieval methods suggested by other authors (Paganin et al., 2002).

Fig. 5A–D displays the results obtained with the one-image SPCI treatment when applied to gold nano-particles images recorded at defocus $\Delta z = -20$ nm. Similarly, the same treatment was applied to an image recorded at defocus $\Delta z = +60$ nm in Fig. 5E–H.

The image in Fig. 5B recorded at $+60$ nm is characterized by a poor quality in comparison with the one recorded at -20 nm defocus (Fig. 5A). However, the related phase image retrieved with the one-image SPCI treatment (Fig. 5B–D and F–H) shows that regardless of the quality of the starting images significant contrast enhancement and noise reduction can be obtained. Similar to the two-images SPCI treatment the choice of the Tikhonov parameter is critical to highlight the object of interest. Moreover, comparison with the two-images SPCI results (Fig. 4), the one-image SPCI treatment is efficient in terms of contrast enhancement and noise reduction. Due to the facility of use and the short computation time, the one-image SPCI treatment should be appropriate to improve low-contrast images produced by biological preparation as we reported in the next section.

4.2.2. Application on biological samples

We have evaluated the efficiency of the one-image SPCI treatment on images from frozen hydrated *E. coli*. It must be taken into account that, due to the object size, the defocus required for biological samples is far from the nanometric scale and frequently goes to 1 or 2 µm. Fig. 6 displays images corresponding to a focus of $+2.496$ µm and -2.496 µm. These images do not provide any information about heterogeneity in bacterial cytoplasm. Furthermore, relative to intensity profiles (Fig. 6E), it is not possible to distinguish the border of the bacterial wall. When the two-images SPCI treatment (Tikhonov parameter a-value $= 0.0085\,\mathrm{nm}^{-1)}$, is applied to two focused $\pm$ 2.496 µm images, the border of the bacteria becomes visible (Fig. 6C) as demonstrated by the *minima* observed in the corresponding plot profile (Fig. 6E, arrows). With the one-image SPCI treatment (Tikhonov parameter a-value $= 0.0085\,\mathrm{nm}^{-1}$) the retrieved phase image and the corresponding profile shows that, not only the borders of the bacteria appears clearly visible, but some details are also distinguishable within the cytoplasm (Fig. 6D and E). According to the plot profile, four regions can be distinguished: the region outside of the bacteria, the bacterial cell wall (Fig. 6E, arrows), a region close to the cell wall with higher densities (Fig. 6E, brackets) and the inner cytoplasm (Fig. 6E). The region close to the cell wall could be the presence of genetic material that it is known to be close to the membrane in bacteria (Leibowitz and Schaechter, 1975); because of the chemical composition of the DNA, may generate a higher phase value. This result illustrates how the one-image SPCI treatment can help to highlight information otherwise invisible in the original data.

To further evaluate the one-image SPCI treatment interest, we compared it with the widely used Fourier band-pass filter. On a TEM image of an epon embedded section of *E. coli*, although the mitochondrion is identifiable (Fig. 7A), it is no possible to clearly distinguish the cristae due to the low contrast and noise. A Fourier band-pass filter (12–24 nm) enables to enhance mitochondrial borders as show in Fig. 7B. The one-image SPCI treatment gives a phase image (Fig. 7C) where the mitochondria borders are well preserved and the main densities occurring in the mitochondrial lumen can be interpreted as cristae (yellow arrows in Fig. 7).

This example illustrates the differences in filtering operated by a band-pass filter compared with the one-image SPCI treatment. This is accounted by the fact that the band-pass filter evenly transmits all frequencies within the interval defined by the low and high frequencies while the one-image SPCI treatment filtering is described by the Tikhonov function $T(q)$ (Fig. 1). In the present case, the latter is more appropriate as it provides just the right amount of details. It also allows for a better segmentation as illustrated by the color image in Fig. 7D. In other word, the one-image SPCI treatment prevents effects that can be generated by a Fourier band-pass filter whilst enhancing the borders of the objects.

5. Discussion

In the last decades, there has been increasing need for TEM use for the characterization of biologicals and materials science. This has led to new generations of TEM equipments with lens corrector for sub-Ångström resolution, and to the development of powerful imaging techniques like electron holography and electron tomography. However, to take full advantage of those technological progresses, TEMs require to be operated by highly qualified experts and accurate results can only be obtained after preliminary investigations. In that context, it seems particularly relevant to develop approaches

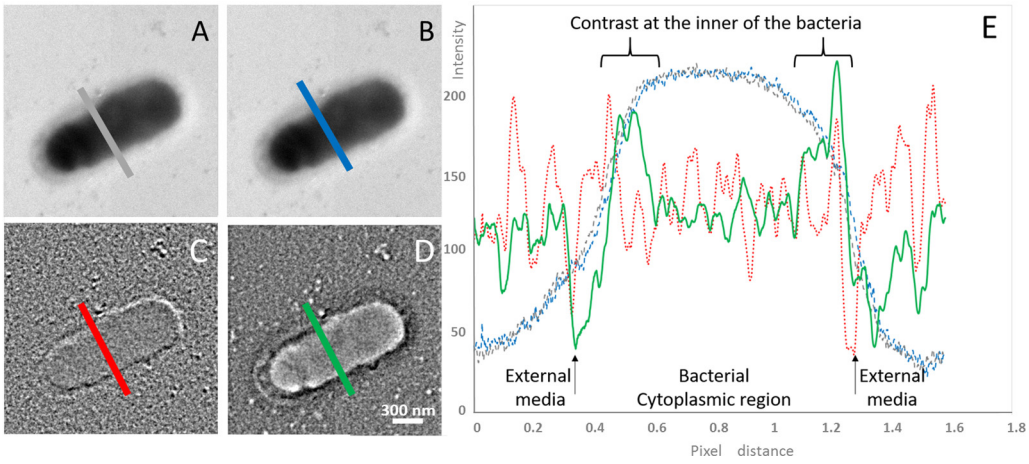

Fig. 6. Comparison of two-images and one-image SPCI treatments in *E. coli* observed by cryo-TEM. (A and B) Raw images acquired at −2.496 µm and +2.496 µm of defocus respectively. (C) Phase image obtained with the two-images SPCI treatment with Tikhonov parameters: $a = 0.0085\,\mathrm{nm}^{-1}$. (D) Phase image obtained using the one-image SPCI treatment with image A and the same Tikhonov *a*-value. Graph E corresponds to intensity profiles of the bacteria *E. coli*. These profiles are recorded along the line of interest across the bacteria as drawn on the TEM images and phase images. Blue and grey lines represents raw focused images, dotted red line to two-images treatment and green line to one-image treatment. In this last one arrows point at the bacterial cytoplasmic region close to borders. Scale bar is 300 nm.

achievable on standard equipment and involving simple numerical treatments in order to be fully carried out and understood by the TEM user. That was the purpose of the work reported here.

In the present manuscript, we have shown that it is possible to propose a simple image treatment based on two defocused images, or even on one defocused image, applicable to phase-contrast images classically acquired in TEM. This image treatment is a simple derivation based on the contrast transfer function. It allows the retrieval of a phase image with a clear view of the underpinning approximation. Therefore, the limits in terms of resolution and quantitative measurements are easy to be defined by the average TEM user.

One main result of this work has been the development of a public ImageJ plugin, SPCI, which can be downloaded from (Verguet, 2018). The strength of SPCI is to involve a single adjustable parameter (the Tikhonov regularization parameter *a*-value). The plugin dialog box gives the possibility to vary the *a*-value over a wide range and to display as many images as applied parameters. This is very convenient for the user to make the most appropriate choice of the *a*-value for contrast enhancement in non-quantitative studies. Also, as demonstrated by the gold particles example, the two-images SPCI treatment is able to provide accurate quantitative results as far as it is applied with the smallest Tikhonov parameter. This requirement can be understood from the description of the Tikhonov function given in Section 2. The deviation of the Tikhonov function to the $1/q^2$ function gives an indication of the frequency domain from which artifacts may arise. This means that depending on the image characteristics (mainly the long-range contrast fluctuation) the two-images SPCI treatment will provide semi-quantitative results. Ideally, images with no long-range contrast fluctuation should allow for a quantitative use of the phase map. This is what we have observed with the gold nano-particles examples when the minimum possible value is used.

Since the choice of the smallest size for the Tikhonov parameter, is required for quantitative studies, this choice becomes obvious since the image manipulation is performed in pixel units (*i.e.* it means taking 1 pixel). Actually in addition to the pixel number indicated in the dialog box, the value of a can be tuned by changing the acquisition conditions since the size of a pixel in the reciprocal space (*i.e.* $1/Np$) depends on them. It is worth noticing that reducing the magnification allows to

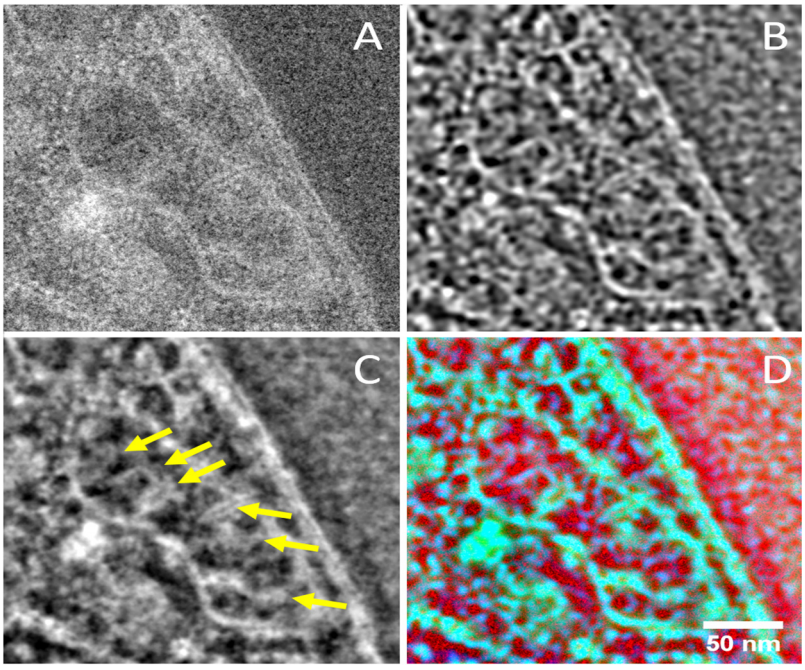

Fig. 7. Comparison of one-image SPCI treatment versus band-pass filter in the identification of mitochondrion cristae. (A) Raw image defocused at +83 nm. (B) Band-pass filtered image (frequencies corresponding to 12–24 nm in real space which heuristically highlight sub-cellular structures in this sample). (C) Phase image resulting from one-image SPCI treatment with a Tikhonov parameter of $0.012\,\mathrm{nm}^{-1}$. The cristae, identified by yellow arrows, appears clearly visible. (D) Overlapping of the previous images with raw image in red channel, band-pass filtered image in blue channel and one-image SPCI-phase image in green channel. Of note, the small red dots, corresponding to high frequency noise, occur all over the image. These dots are removed by both band-pass and one-image SPCI treatment. However, it should be noticed that the band-pass is associated with artifacts depicted by the blue densities that are absent in the SPCI green image. Scale bar is 50 nm.

explore small values of a which can be out of reach with high magnification. The interest of the a-value in pixels is to realize how far the chosen parameter is from the minimum value for the given acquisition condition. Because of the a-value in nm^{-1} the operator has a direct information on the length scale that will be enhanced by the Tikhonov regularization. As a consequence, it makes easier for the user to understand how the experimental conditions should be changed. Typically, the magnification should be chosen in order that the meaningless information, such as the scale of the long-range contrast fluctuation, is as large as possible with respect to the image size while the meaningful details remain small with respect to the image size.

As the SPCI plugin offers two possible modes, their respective limits and advantages have to be discussed. At first the choice for the one-image or two-images SPCI treatment depends on the needs of qualitative or quantitative information. If a qualitative information is desired, the two-images SPCI treatment should be performed. Indeed, the one-image treatment can be quantitative as long as the first requirement of knowing the zero-defocus image is fulfilled. To avoid any misuse, it is explicitly indicated on the dialog box that the one-image SPCI treatment is not a quantitative approach. If the sample is a weak phase object, the zero-defocus image is recognized by its absence of contrast. Unfortunately, this zero contrast may be difficult to observe because of small local effects of diffraction and/or absorption, and also because the sample may not be flat. As a consequence, the errors on the focus value and the zero-focus image prevent from using the one-image SPCI treatment for phase measurement. However, it must be said that phase retrieval can be performed on the basis of a single image and it has been successfully applied in X-ray (Paganin et al., 2002) and TEM (Liu et al., 2011) imaging. This was possible due to the sophisticated reconstruction algorithms and when dealing with homogeneous and simple objects. However, the objective of the present work is to propose the simplest approach even at the expense of spatial resolution of quantitative phase information, provided that the users have a clear understanding of the methodological limits.

If a qualitative information is desired, for instance when the characterization of an object's size and shape are of interest, the images obtained with the one-image SPCI treatments can be exploited. In that case, the one-image SPCI treatment provides images with a significant gain of contrast facilitating automatic segmentation by simple thresholding. From that point of view, the one-image treatment is clearly advantageous on the two-images one. First with the one-image treatment, image alignment is not necessary. Therefore, there is no risk of artifact on the object size due to too ill corrected misalignment. This is particularly important for biological samples as they require high defocus inducing specific image distortion preventing from good alignment of the two images focal series. Also even if the two-images SPCI treatment is chosen in view of quantitative results, the one-image SPCI treatment is always worth doing in order to detect artifact due to incorrect image alignment. This is a preliminary step required for shape descriptors and dimension studies, which can be directly performed in the ImageJ software where SPCI plugin has been implemented.

As illustrated in Section 4, the one-image SPCI treatment can be seen as a type of band-pass filter. The filtering functions are also significantly different: a top hat shape in reciprocal space for the band-pass filter and a kind of bell shape for the Tikhonov function. As a consequence, the band-pass filter requires to adjust two parameters while the Tikhonov function has only one adjustable parameter. One shape or the other might be more appropriate depending on the spatial frequency characteristic of the system of interest as illustrated by Fig. 7. Additionally, since the SPCI plugin allows for trying and displaying the results obtained for several a-values, it is rather easy to determine the optimum conditions in a single run. Second, although the phase image given by the one-image SPCI treatment cannot be quantitative, there is still a direct connection between the one-image SPCI treatment and the phase-contrast, while a band-pass filter is applicable to any types of image regardless of the contrast used to form the image. This means that the phase image given by the one-image SPCI treatment still bears a physical meaning related to the phase-contrast.

With the development of techniques like electron holography or holo-tomography and of devices like phase plates, phase-contrast information appears as extremely relevant in material sciences and biology. Therefore, the one-image SPCI treatment can appear quite fruitful despite its limits. For instance, it might be beneficial for beam sensitive systems, such as frozen hydrated samples in biology, or in material science systems in which electron holography or holo-tomography could be of interest but appear unfeasible. Of course, the one-image SPCI treatment cannot be an alternative to these techniques. We only propose to use it when advanced methods cannot be carried out or in a preliminary investigation to these advanced techniques. Also considering the growing interest of phase plates for biological system, images bearing phase information may be of specific interest even though they cannot be quantitative in terms of phase measurements.

6. Conclusion

To summarize, we propose here a plugin which gives the possibility to retrieve phase images from TEM phase-contrast images obtained with standard microscopes by users not specialized in electron optics. Depending on the needs and the system, a quantitative approach (*i.e.* using two symmetric focused images) or a qualitative approach based on a single image is possible. The aim of this plugin is to make phase retrieval possible at a basic level as a preliminary investigation prior to accurate studies on specialized microscopes. Alternatively, the qualitative application of the plugin can be of interest as a new image processing able of selective contrast enhancement. For example, it can be useful for the study of the low contrasted objects specifically frequent in cryo TEM of biological systems.

Acknowledgment

We are grateful to Prof. G.A. Botton from CCEM-Canadian Center for Electron Microscopy for the nano-particle imaging facilities and to Sylvain Trépout for the *T. brucei* grid and the critical reading of the manuscript. We acknowledge the PICT-IBISA for providing access to their image equipment. A. Verguet is recipient of a CIFRE grant and is supported by JEOL (Europe) SAS.

References

Donnadieu, P., Lazar, S., Botton, G.A., Pignot-Paintrand, I., Reynolds, M., Perez, S., 2008. Seeing structures and measuring properties with transmission electron microscopy images: a simple combination to study size effects in nanoparticle systems. Appl. Phys. Lett. 94. https://doi.org/10.1063/1.3168525. ISI:000267697300053.

Ishizuka, K., Allman, B., 2005. Phase measurement of atomic resolution image using transport of intensity equation. J. Electron Microsc. 54, 191–197. https://doi.org/10.1093/jmicro/dfi024.

Karuppasamy, M., Nejadasl, F.K., Vulovic, M., Koster, A.J., Ravelli, R.B.G., 2011. Radiation damage in single-particle cryo-electron microscopy: effects of dose and dose rate. J. Synchrotron Radiat. 18, 398. https://doi.org/10.1107/S090904951100820X.

Koch, C.T., 2014. Towards full-resolution inline electron holography. Micron 63, 69–75. https://doi.org/10.1016/j.micron.2013.10.009.

Leibowitz, P.J., Schaechter, M., 1975. The Attachment of the Bacterial Chromosome to the Cell Membrane. Int. Rev. Cytol. 41, 1–28. https://doi.org/10.1016/S0074-7696(08)60964-X.

Liu, A.C.Y., Paganin, D.M., Bourgeois, L., Nakashima, P.N.H., 2011. Projected thickness reconstruction from a single defocused transmission electron microscope image of an amorphous object. Ultramicroscopy 111, 959–968 doi: 10.1016/j.ultramic.2011.03.007.

Messaoudi, C., Boudier, T., Sorzano, C.O.S., Marco, S., 2007. TomoJ: tomography software for three-dimensional reconstruction in transmission electron microscopy. BMC Bioinform. 8, 288. https://doi.org/10.1186/1471-2105-8-288.

Messaoudi, C., 2011. TomoJ. URL: https://sourceforge.net/projects/tomoj (Online; accessed 27.11.2018).

Mitome, M., Ishizuka, K., Bando, Y., 2010. Quantitativeness of phase measurement by transport of intensity equation. J. Electron Microsc. 59, 33–41. https://doi.org/10.1093/jmicro/dfp046.

O'Keefe, M.A., Hetherington, C.J.D., Wang, Y.C., Nelson, E.C., Turner, J.H., Kisielowski,

C., Malm, J.O., Mueller, R., Ringnalda, J., Pan, M., Thust, A., 2001. Sub-Ångstrom high-resolution transmission electron microscopy at 300 keV. Ultramicroscopy 89, 215–241. https://doi.org/10.1016/S0304-3991(01)00094-8.

Paganin, D., Nugent, K.A., 1998. Noninterferometric phase imaging with partially coherent light. Phys. Rev. Lett. 80, 2586–2589. https://doi.org/10.1103/PhysRevLett.80.2586.

Paganin, D., Mayo, S.C., Gureyev, T.E., Miller, P.R., Wilkins, S.W., 2002. Simultaneous phase and amplitude extraction from a single defocused image of a homogeneous object. J. Microsc. 206, 33–40. https://doi.org/10.1046/j.1365-2818.2002.01010.x.

Popescu, R., Müller, E., Wanner, M., Gerthsen, D., Schowalter, M., Rosenauer, A., Bóttcher, A., Lóffler, D., Weis, P., 2007. Increase of the mean inner Coulomb potential in Au clusters induced by surface tension and its implication for electron scattering. Phys. Rev. B 76, 235411. https://doi.org/10.1103/PhysRevB.76.235411.

Reimer, L., 1989. Transmission Electron Microscopy – Physics of Image Formation and Microanalysis. Springer. URL: https://www.springer.com/de/book/9783662215791.

Schiske, P., 2002. Image reconstruction by means of focus series. J. Microsc. 207, 154. https://doi.org/10.1046/j.1365-2818.2002.01042.x.

Schneider, C.A., Rasband, W.S., Eliceiri, K.W., 2012. NIH image to ImageJ: 25 years of image analysis. Nat. Methods 9, 671. URL: https://imagej.nih.gov/ij (pMID: 22930834).

Thevenaz, P., Ruttimann, U.E., Unser, M., 1998. A pyramid approach to subpixel registration based on intensity. IEEE Trans. Image Process. 7, 27–41. https://doi.org/10.1109/83.650848.

Trémeau, A., Schettini, R., Tominaga, S., 2009. Computational Color Imaging. Springer Berlin Heidelberg.

Trépout, S., Tassin, A.M., Marco, S., Bastin, P., 2018. STEM tomography analysis of the trypanosome transition zone. J. Struct. Biol. 202, 51–60. https://doi.org/10.1016/j.jsb.2017.12.005.

Tseng, Q., 2018. Template Matching and Slice Alignment, ImageJ Plugins. URL: https://sites.google.com/site/qingzongtseng/template-matching-ij-plugin (Online; accessed 27.11.2018).

Van Dyck, D., Lichte, H., van der Mast, K.D., 1996. Sub-ångström structure characterisation: the Brite–Euram route towards one ångström. Ultramicroscopy 64, 1–15. https://doi.org/10.1016/0304-3991(96)00057-5.

Verguet, A., 2018. SPCI Plugin Distribution. URL: http://www.cmib.fr/en/download/softwares/SPCI.html (Online; accessed 27.11.2018).

Wendykier, P., Nagy, J.G., 2010. Parallel colt: a high-performance Java library for scientific computing and image processing. ACM Trans. Math. Software 37, 1–22. https://doi.org/10.1145/1824801.1824809.